

Ion heating in the presheath

Albert Meige,^{a)} Orson Sutherland, Helen B. Smith, and Rod W. Boswell

Space Plasma Power and Propulsion Group, Research School of Physical Sciences and Engineering,
Australian National University, ACT 0200, Australia

(Received 12 December 2006; accepted 23 January 2007; published online 19 March 2007)

A one-dimensional model of a small plasma ion source (10 cm long) is studied. A hybrid simulation where ions are treated as particles and electrons as a fluid obeying the Boltzmann relation is used to investigate ion heating in the plasma presheath. At low pressure (below a few mTorr), the ion velocity distribution is Maxwellian in the bulk and becomes a drifting Maxwellian distribution while transiting the presheath. The distribution remains essentially isotropic as the ions are accelerated through the presheath to satisfy the Bohm criterion. At intermediate pressures (around 10 mTorr), ion-neutral collisions scatter a significant part of the ion kinetic energy from the parallel direction to the perpendicular direction, leading to a net heating of the ions. In addition, the ion velocity distribution becomes distinctly anisotropic. At higher pressure (above a few tens of mTorr), ion heating is still observed, but yields isotropic ion velocity distributions. © 2007 American Institute of Physics. [DOI: 10.1063/1.2709648]

I. INTRODUCTION

For a plasma contained in a vacuum vessel with insulating walls or metallic walls where a current does not flow, a steady state can only be maintained if equal amounts of positive and negative charge flow to each area element of the walls. As the electrons are typically 100 times hotter than the ions, an electric field must exist between the neutral plasma and the wall in order to retain the electrons and accelerate the ions. This nonneutral (positive) region balancing the electron and the ion flux is called the *sheath*. Sheaths are one of the most prominent and well-known features of confined plasmas as they are critical in many situations, for example, in providing a directed ion energy for directional etching in the fabrication of semiconductor devices.

The typical width of the sheath is on the order of a few Debye length and is generally small compared with the other characteristic lengths of the plasma such as the ion mean free path. However, this typical situation leads to complications as the significant distortion of the ion distribution due to the wall losses prevents the formation of a stable sheath unless ions enter it with a critical minimum velocity that is much greater than the thermal velocity. This condition is known as the *Bohm criterion*. Ions can reach this critical velocity thanks to the existence of a transition layer, the so-called *presheath*, between the sheath and the neutral plasma where a small electric field accelerates the ions.

In a very interesting review paper, Riemann¹ gives an overview of the history of the discovery of both the sheath and the presheath. In summary, the basic features of the plasma-sheath transition (the presheath) was introduced implicitly by Langmuir² and in the famous ground-breaking paper by Tonks and Langmuir.³ Bohm⁴ was the first to give an explicit formulation and a clear interpretation of the

sheath condition in the collisionless case and showed that the ions had to enter the sheath with at least the ion sound speed $(k_B T_e / m_i)^{1/2}$, where k_B is the Boltzmann constant, T_e the electron temperature, and m_i the ion mass. Harrison and Thompson⁵ have solved the Tonks-Langmuir problem analytically and found a much more general formulation of the Bohm criterion. Riemann⁶ gave the first self-consistent analysis of a collisional presheath. Finally, the term *presheath* itself was first introduced by Hu and Ziering⁷ and the nomenclature was clarified by Franklin⁸ and Riemann.⁹ It was shown analytically by Riemann,¹⁰ and experimentally by Oksuz and Hershkovitz,¹¹ that the size of the presheath scales like $\lambda_{\text{mfip}}^{1/5} \lambda_D^{4/5}$, where λ_{mfip} and λ_D are the ion mean free path and Debye length, respectively.

At ion energies greater than about 1 eV ion-neutral collisions can be viewed as simply an electron jumping from a stationary atom to the transiting ion without any perturbation to the trajectories. For ion energies less than about 0.2 eV, the electric field of the approaching ion tends to polarize the stationary atom and the two will start to orbit each other, resulting in a more and more isotropic collision (in the center-of-mass frame). Hence as the ions are accelerated by the presheath electric field, they are initially “locked” to the neutrals that surround them and the energy they gain from the field appears as a heating of both the ion population and the local neutrals. Further increases in the ion energy are accompanied by a reduction in the polarization effect as the transit period decreases and the ions “run away” from the neutral population. In the present study we will investigate this ion heating effect in the presheath, in particular how the perpendicular temperature is affected. As well as being an interesting issue as such, perpendicular heating of the ions in the presheath is also a fundamental issue in applied plasma physics, for example, for etching, where the ion angular distribution function is critical for the shape of the trenches or for focused ion beams, where the ultimate brightness of plasma is limited by the ion perpendicular temperature.

^{a)}Present address: Laboratoire de Physique et Technologie des Plasmas (LPTP), Ecole Polytechnique, Palaiseau Cedex 91128, France. Electronic mail: meige@ltp.polytechnique.fr

We use a hybrid simulation where ions are treated as particles and electrons as a fluid obeying the Boltzmann relation to investigate ion heating and ion transport through the presheath. Some of the work reported here presents similarities with the work originally performed by Smith,¹² who used the full particle-in-cell simulation XPDP1 developed in Berkeley.¹³ However, in the present work, we use a different scheme to treat the important ion-neutral collisions and the hybrid simulation was run at higher, more realistic plasma densities. Despite these significant differences, we find the same trends as those of Smith, hence, confirming the original study. Some of Smith's results were also reported by Sutherland.¹⁴

II. MODEL

A. Hybrid model

If electrons are assumed to be in Boltzmann equilibrium *a priori*, the electron plasma frequency does not have to be resolved by the time step of the simulation. This allows the use of much larger time steps than with the full classical particle-in-cell scheme, significantly reducing computational cost and therefore time to convergence.

The hybrid simulation developed here follows the same basic algorithm as a standard particle-in-cell simulation^{15,16} and is described in detail in Ref. 17. In short: (i) the charges are accumulated on the mesh, (ii) Poisson's equation is solved to find the corresponding electric field, and (iii) Newton's law is used to accelerate the particles according to the electric field. These steps constitute one iteration and iterations are repeated until the simulation reaches steady state. Since electrons are assumed to be in Boltzmann equilibrium their density n_e is given by

$$n_e = n_0 \exp \frac{e\Phi}{k_B T_e}, \quad (1)$$

where n_0 is the electron density at the point where the potential Φ is null, T_e is the electron temperature, and k_B is the Boltzmann constant.

Poisson's equation is coupled with the Boltzmann relation in the following way. Let upper indices refer to a moment in time and let Δt be a time step, with $t^{k+1} = t^k + \Delta t$, assuming that the value of the quantities are known at t^k and are to be calculated at t^{k+1} .

Poisson's equation reads

$$\left(\frac{\partial^2 \Phi}{\partial x^2} \right)^{k+1} = - \frac{\rho}{\epsilon_0} = - \frac{e}{\epsilon_0} (n_i^k - \tilde{n}_e^{k+1}), \quad (2)$$

where n_i^k is the ion density coming from the accumulation of the particle ion charges on the mesh. To avoid numerical instabilities, a first-order estimate of the electron density \tilde{n}_e^{k+1} (function of Φ^k and Φ^{k+1}) at t^{k+1} is used. The spatial integration of Eq. (2) is performed following any classical algorithm for solving tridiagonal systems (Ref. 18, for example). In hybrid models, the electron density reference n_0 is commonly imposed or hidden in normalization of variables. Imposing n_0 can lead to a miscalculation of the sheath potential and can therefore lead to errors in the calculation of plasma

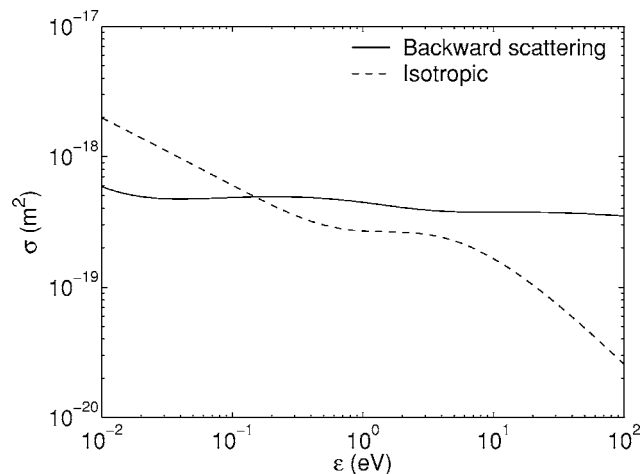


FIG. 1. Ion-neutral collision cross sections σ as a function of energy \mathcal{E} , recommended by Phelps (Ref. 20). The ion kinetic energy \mathcal{E} is in the laboratory frame, the neutral target being at rest.

parameters. In the present work, the density reference n_0 is self-consistently calculated at every time step; this is done by estimating the real electron flux to the walls and an electron balance within the plasma (accounting for electron loss and creation). Details for the calculation of n_0 can be found in Refs. 17 and 19.

At each time step, a number of new ions are introduced into the simulation, with a spatial distribution following the electron density. The initial velocity of the new ions is taken from a Maxwellian distribution at room temperature ($T_{\text{room}} = 0.026$ eV).

B. Ion-neutral collisions

We wish to investigate the possible increase of the temperature of the ions in the direction perpendicular to their motion through the presheath. Hence, ion-neutral collisions are a particularly important phenomenon to model, as they will be responsible for the transfer of momentum and energy from the parallel to the perpendicular direction. For the present study, the recipe recommended by Phelps²⁰ was followed.

Phelps²⁰ recommends not to treat elastic and charge exchange collisions as independent events. Instead, an isotropic component (in the center-of-mass frame) and a backward peaked component (rotation of π in the center-of-mass frame), with the appropriate and accurate collision cross sections,²¹ are used and shown in Fig. 1.

We use the *null-collision* method²² to choose among the various collision events. At each time step, a number of test ions are randomly selected. In the *null-collision* approach, this number is greater or equal to the maximal number of collisions that may occur within a time step. For each of these test ions, the velocity of a neutral is taken from a three-dimensional Maxwellian distribution at room temperature. The relative ion-neutral velocity and kinetic energy are calculated to determine the collisional event undergone. The actual collision is either isotropic, backward scattering, or nothing (null collision). Once the occurrence and type of a collision is known, the ion is transferred into the center-of-

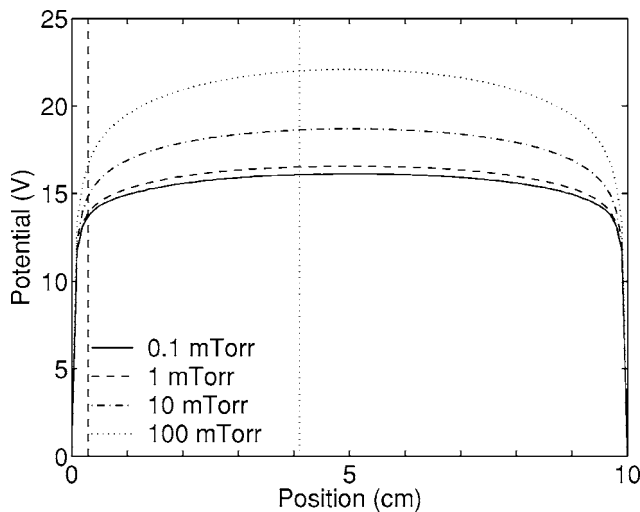


FIG. 2. Plasma potential profiles as a function of position for various pressures ranging from 0.1 to 100 mTorr. The vertical dashed and dotted lines show the sheath-presheath boundary and the bulk-presheath boundary, corresponding to the 10 mTorr case, respectively.

mass frame, undergo the collision (isotropic elastic or backward scattering) and is transferred back into the laboratory frame. Note that other ion-neutral models have been proposed (Refs. 23 and 24, for example), however, Phelps's model appears to be a good compromise between accuracy and computational efficiency.

The simulations model a 10-cm-long inductive argon discharge in line with the experimental device referred to in the Introduction and are allowed to run for several milliseconds in order to reach a high degree of convergence. In order to sufficiently resolve the tail of the distributions, the number of macroparticles used is between 2×10^5 and half a million, with 250 cells along the x axis and a time step of 10^{-8} s. The electron temperature is 3 eV, unless stated otherwise, and the plasma density between 4×10^{16} and $3 \times 10^{17} \text{ m}^{-3}$, depending on the neutral pressure. Finally, it should be noted that in all the results presented here, the conditions of pressure, plasma density, and electron temperature are such that the Debye length λ_D is very short compared to the ion mean free path λ_{mfip} . In other words, the sheath is essentially collisionless.

III. RESULTS

A. Basic analysis at 10 mTorr

The dashed-dotted line in Fig. 2 shows the plasma potential profile as a function of position for a neutral pressure of 10 mTorr. The vertical dashed and dotted lines show the sheath-presheath boundary and the bulk-presheath boundary, respectively. Although at low pressure, when both the sheath and the presheath are collisionless, the sheath-presheath boundary and the bulk-presheath boundary can be rather clearly defined, this is not the case at higher pressure, when the ions are relatively collisional. For collisional plasmas, the bulk and the presheath merge and the exact position of the sheath is a matter of definition.²⁵ In the following, the term *presheath* may be used loosely and what is meant is the

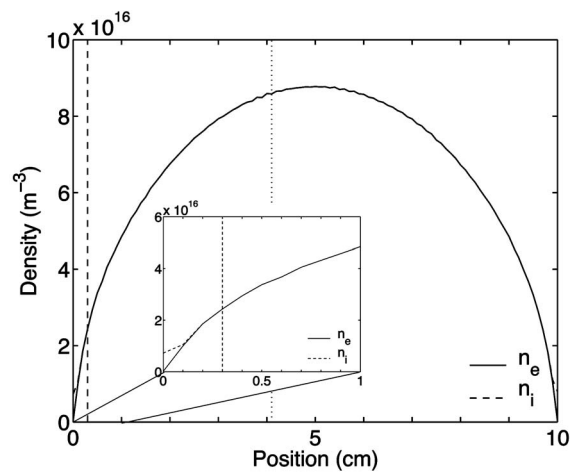


FIG. 3. Electron (solid line) and ion (dashed line) density profiles as a function of position for a neutral gas pressure of 10 mTorr. The vertical dashed and dotted lines show the sheath-presheath boundary and the bulk-presheath boundary, respectively. The breakdown of the plasma quasineutrality defines the sheath-presheath boundary.

whole accelerating electric field existing between the field-free region (the bulk) and the sheath. The exact boundaries that were chosen for the presheath are detailed in the following two paragraphs.

Figure 3 shows both the electron (solid line) and ion (dashed line) density profiles corresponding to the 10 mTorr case. The quasineutrality of the plasma holds rather well in the whole discharge, except in the sheath where it breaks down, as shown in the insert representing a zoom of the sheath region. The sheath-presheath boundary is taken where the quasineutrality of the plasma breaks down, i.e., where the relative electric charge $\Delta n/n$ exceeds 10%. This position also corresponds to the point where the Bohm velocity is reached. The sheath-presheath boundary of the 10 mTorr case is shown by the vertical dashed line.

The dashed-dotted line in Fig. 4 shows the ion mean kinetic-energy profile of the 10 mTorr case. As expected, the ion mean energy increases from the center of the discharge to the walls as a result of the ions being accelerated by the presheath and later by the sheath. The ion mean energy in the center of the discharge (bulk) is approximately $\mathcal{E}_{\text{bulk}} = 0.045$ eV, which corresponds well with room temperature ($\mathcal{E}_{\text{bulk}} \sim 3/2T_{\text{room}}$). This shows that in the center of the discharge, where the electric field almost vanishes, ions have essentially the same energy as neutrals, on account of the large mass ratio between neutrals and ionizing electrons. However, the electric field is not zero, except at the exact center of the discharge, and a small field accelerates ions towards the walls. The transition between the bulk plasma and the presheath is not obvious in Figs. 2–4, hence the bulk-presheath boundary is defined to be the position where the bulk ions have gained more than 10% of their initial energy, when accelerated by this small field. The position of this boundary (10 mTorr case) is shown by the vertical dotted lines in the figures already mentioned. It should be noted that our definition of the presheath may be different from the

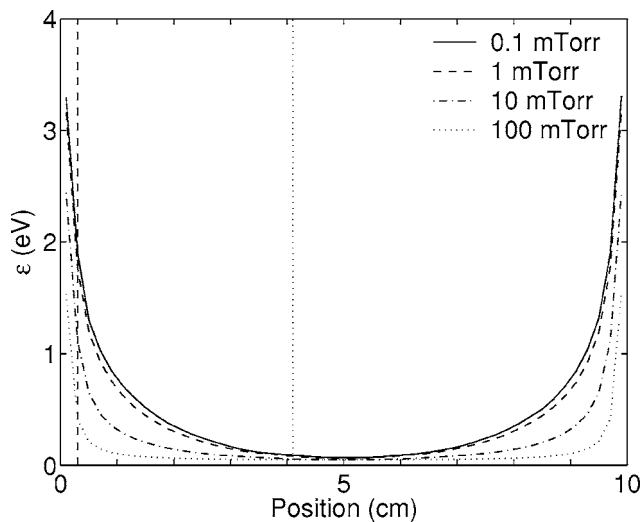


FIG. 4. Ion mean kinetic-energy profiles as a function of position for various pressures ranging from 0.1 to 100 mTorr. The vertical dashed and dotted lines show the sheath-presheath boundary and the bulk-presheath boundary, respectively. A 10% increase of the ion mean energy from the bulk ion energy (center of the discharge) defines the bulk-presheath boundary.

“standard” definition, but once again this is because we wish to investigate the ion heating through the whole accelerating field (loosely called *presheath* in this paper).

The ion mean kinetic energy averaged over the presheath length is ~ 0.2 eV. Hence, the isotropic and backward scattering collision cross sections are $\sigma_{is} \sim 42 \text{ \AA}^2$ and $\sigma_{bs} \sim 49 \text{ \AA}^2$, respectively. For a neutral pressure of 10 mTorr, the neutral gas density is $n_n \sim 3.3 \times 10^{20} \text{ m}^{-3}$ at room temperature; this yields a mean free path for ions of

$$\lambda_{mpf} = \frac{1}{(\sigma_{bs} + \sigma_{is})n_n} \sim 3 \text{ mm.} \quad (3)$$

Under these conditions, the presheath is ~ 3.8 cm or approximately 10 ion mean free paths thick according to Eq. (3). Therefore, ions undergo a significant number of collisions during their journey through the presheath and can transfer some of their parallel energy into the perpendicular direction. Note that the size of the presheath mentioned previously may well seem to be very large, but once again, this is a matter of definition of the presheath.

B. Investigating the influence of pressure from 0.1 to 100 mTorr

The definition of the sheath-presheath boundary and of the bulk-presheath boundary are the same as stated previously. Additionally, the perpendicular ion velocity is defined as $v_{\perp} = \sqrt{v_x^2 + v_z^2}$ and the corresponding kinetic energy $\mathcal{E}_{\perp} = 1/2 m_i v_{\perp}^2$, where m_i is the ion mass. Figure 5 shows the perpendicular ion mean energy \mathcal{E}_{\perp} profiles for pressures ranging from 0.1 to 100 mTorr. It is observed from the dashed-dotted line (10 mTorr case) that \mathcal{E}_{\perp} increases from the bulk to the walls. To satisfy the Bohm criterion, the presheath accelerates the ions in the parallel direction from room temperature (in the bulk) to the Bohm velocity. The perpendicular ion mean energy is ~ 0.03 eV in the bulk

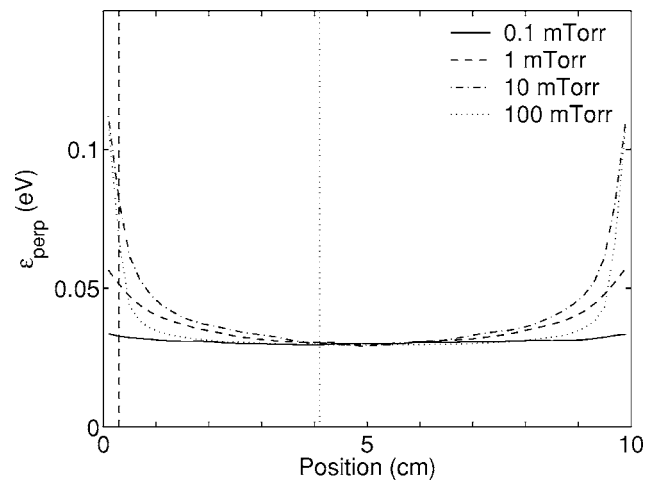


FIG. 5. Perpendicular ion mean energy \mathcal{E}_{\perp} profiles as a function of position for various pressures ranging from 0.1 to 100 mTorr. The vertical dashed and dotted lines show the sheath-presheath boundary and the bulk-presheath boundary, corresponding to the 10 mTorr case, respectively; the limits for other the pressures are slightly different.

(which is 2/3 of the total mean energy as the distribution is isotropic) and ~ 0.07 eV just before entering the sheath. This shows that for a neutral pressure of 10 mTorr, ions are heated in the perpendicular direction up to twice their bulk energy. A possible explanation for the increase of the perpendicular energy is that during their acceleration, ions undergo collisions with neutrals, hence, partially scattering their directed parallel energy to the perpendicular direction; this assumption will be confirmed later. Figure 5 also shows that at very low pressure (0.1 mTorr, solid line), ions are not heated perpendicularly. At much higher pressure (100 mTorr, dotted line), the perpendicular heating in the presheath seems to be less important than at 10 mTorr, suggesting that the perpendicular heating is not a monotonic function of pressure.

Figure 6 shows the potential drop across the presheath as a function of pressure. When the pressure is increased, ions undergo more collisions with neutrals, which reduces their mobility. However, irrespective of the pressure, the Bohm

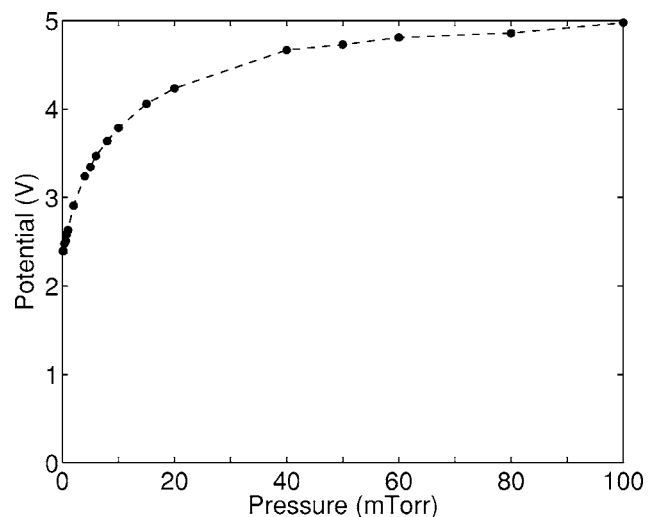


FIG. 6. Potential drop across the presheath as a function of pressure.

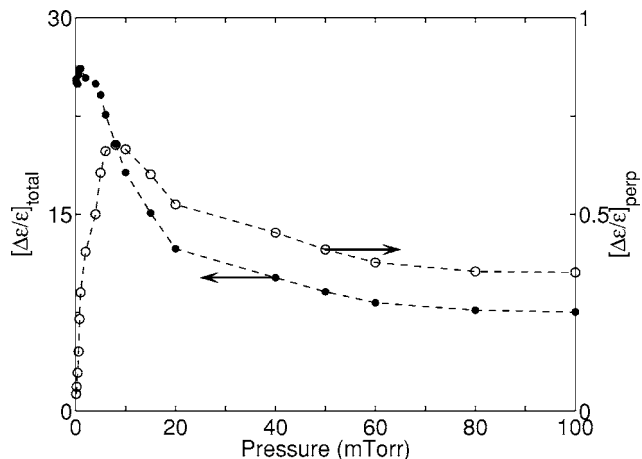


FIG. 7. Ion mean energy relative increase as a function of pressure. The solid circles (\bullet) represent the total kinetic energy (left axis), while the open circles (\circ) represent the perpendicular energy (right axis).

criterion (or its equivalent for collisional plasmas) still holds and the ions must reach a critical velocity before entering the presheath. Hence, the potential drop across the presheath has to increase with the pressure to balance the ion lack of mobility. This trend is observed in Fig. 6, where the potential drop across the presheath is around 2.4 eV at low pressure (0.1 mTorr) and almost 5 eV at higher pressure (100 mTorr). The increase of the potential drop is not linear with pressure and tends to saturate for pressures above 50 mTorr. Note that the critical velocity to be reached by ions before entering the sheath corresponds to the Bohm velocity in the collisionless case; however, at higher pressure, the ion drift lies somewhat below the Bohm velocity (Ref. 26, p. 173 and references therein).

Figure 7 shows the relative kinetic energy gained by the ions when traveling through the presheath as a function of pressure. The relative energy gain is defined by $\Delta\mathcal{E}/\mathcal{E} = (\mathcal{E}_{\text{sp}} - \mathcal{E}_{\text{bulk}})/\mathcal{E}_{\text{bulk}}$, where \mathcal{E}_{sp} and $\mathcal{E}_{\text{bulk}}$ are the ion kinetic energies at the sheath-presheath boundary and at the bulk-presheath boundary, respectively. $[\Delta\mathcal{E}/\mathcal{E}]_{\text{total}}$ represents the total energy increase (solid circles, left axis), while $[\Delta\mathcal{E}/\mathcal{E}]_{\perp}$ represents the perpendicular energy increase (open circles, right axis). Although the potential drop across the presheath increases with pressure (Fig. 6), the total kinetic energy gained by the ions while traversing the presheath decreases with pressure as a result of the decrease of the ion mobility. On the other hand, the perpendicular kinetic energy gained by the ions while traversing the presheath is minimum at very low pressure, a maximum of around 8 mTorr, and follows the same trend as the total kinetic energy for pressures above 20 mTorr. At 8 mTorr, the relative perpendicular energy gain is almost 70% ($\mathcal{E}_{\text{sp}} \sim 1.7 \times \mathcal{E}_{\text{bulk}}$). Above a few tens of mTorr, and within the range of pressures investigated, the perpendicular heating remains significant and ions can gain as much as 40% of their initial perpendicular energy. This shows that for sufficiently collisional plasmas, ions are not only accelerated through the presheath, but also heated, and that the rate of perpendicular heating is not a monotonic function of pressure.

TABLE I. Ion mean kinetic energy in the presheath ($\langle\mathcal{E}\rangle$ (eV), ion mean free path λ_{mfp} (cm), presheath width w_{ps} (cm), and ratio $w_{\text{ps}}/\lambda_{\text{mfp}}$ for various pressures P (mTorr), perpendicular temperature T_{\perp} (eV) of the hot and cold ion population at the sheath-presheath boundary, ratio of hot population number density to cold population number density at the sheath-presheath boundary $\%_{\text{hot}}$.

P	$\langle\mathcal{E}\rangle$	λ_{mfp}	w_{ps}	$w_{\text{ps}}/\lambda_{\text{mfp}}$	T_{\perp}	$\%_{\text{hot}}$
0.1	0.5	38	4.2	0.1	0.03/0.1	<1%
1	0.4	3.9	4.2	1.1	0.03/0.1	5%
10	0.2	0.45	3.8	84	0.04/0.1	8%
100	0.1	0.05	2.8	56	0.04/0.07	2%

In order to explain the nonmonotonic behavior of the perpendicular heating as a function of the neutral pressure, Table I compares the ion mean free path and the presheath thickness for various pressures. This shows that at very low pressure (0.1 mTorr), the presheath is essentially collisionless. Hence, although ions can acquire a significant energy in the direction parallel to the presheath, this energy cannot be transferred to the perpendicular direction via collisions, which explains why no perpendicular heating is observed at low pressure. At high pressures (above a few tens of mTorr), the presheath becomes extremely collisional, and although collisions can distribute the parallel energy to the perpendicular direction, the collisionality is so high that both parallel and perpendicular directions tend to thermalize at the neutral gas temperature or just slightly above. For moderately collisional plasmas (around 10 mTorr), the mobility of the ions is still important and significant parallel energy can be acquired by the ions when falling through the presheath. This energy is partially transferred to the perpendicular direction by just a few collisions with neutrals, presumably explaining the maximum observed in the perpendicular heating at ~ 8 mTorr (Fig. 7).

Figure 8 shows contour plots of ion velocity distribution functions (IVDFs) for various positions and pressures ranging from 0.1 to 100 mTorr. The plots are taken (i) at the center of the discharge, (ii) in the middle of the presheath, and (iii) at the sheath-presheath boundary. In these figures, due to our definition of v_{\perp} , an isotropic distribution yields an oval whose width is twice its height. First, it should be noticed that in the range of pressures investigated, the IVDFs are always relatively isotropic in the center of the discharge, where the net force felt by the ions vanishes.

At low pressure [0.1 mTorr, Fig. 8(a)], although the IVDF acquires a drift velocity while traveling through the presheath, it remains Maxwellian and isotropic. The drift velocity acquired by the ions at the sheath-presheath boundary corresponds approximately to the Bohm velocity under the present conditions. While the distribution moves through the presheath, its low-energy part becomes slightly more important [this is quite visible in Fig. 8(a) (iii)], which is a consequence of the ions that are created within the presheath and are not accelerated through the whole presheath potential drop.

Above a few mTorr [10 mTorr, Fig. 8(c)], the isotropy of the distribution within the presheath breaks down and the

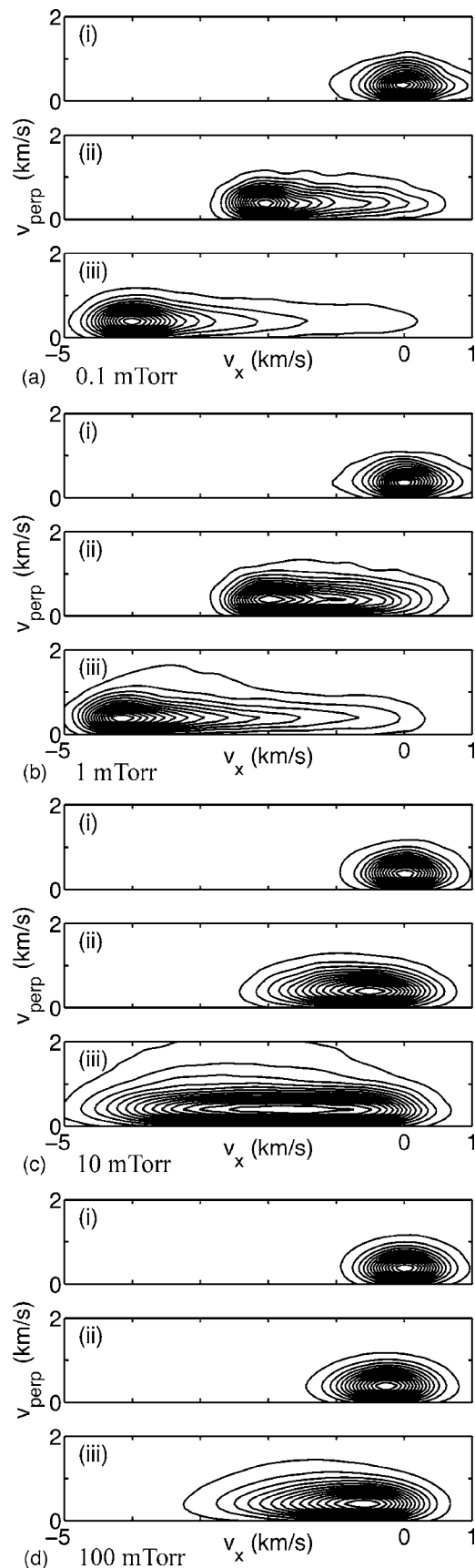


FIG. 8. Contour plots of ion velocity distribution functions (IVDFs) at various positions [(i) bulk, (ii) middle of the presheath, and (iii) sheath-presheath boundary] and for various neutral gas pressures. Abscissas represent parallel velocities and ordinates represent perpendicular velocities v_{\perp} . In these figures, due to our definition of v_{\perp} ($v_{\perp} = \sqrt{v_y^2 + v_z^2}$), an isotropic distribution yields an oval whose width is twice its height.

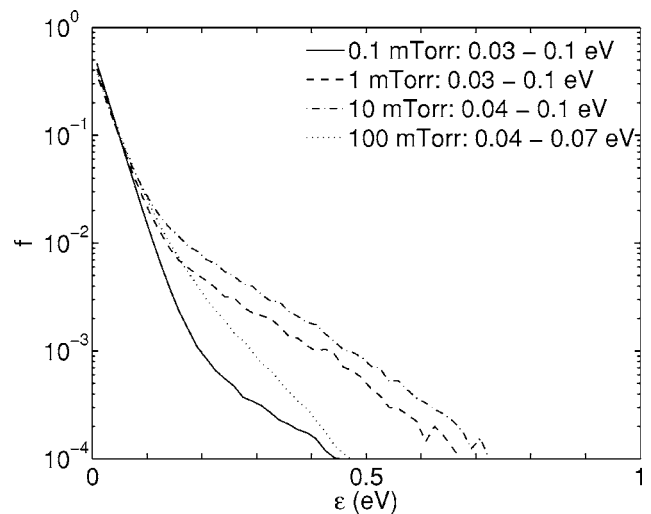


FIG. 9. Perpendicular ion energy distribution functions f at the sheath-presheath boundary for various neutral gas pressures ranging from 0.1 to 100 mTorr. The respective temperatures corresponding to the two distinct distributions of each pressure are indicated on the figure and also summarized in Table I.

distribution becomes wider in both the parallel and the perpendicular directions, indicating that the ions become hotter and not simply faster.

At some tens of mTorr [100 mTorr, Fig. 8(a) (iii)], the average kinetic energy of the ions in the presheath is such that isotropic collisions dominate over backward scattering (Table I and Fig. 1), hence thermalizing the IVDF and making it relatively isotropic. Simulations were run at higher pressures (up to 500 mTorr) and the IVDFs were increasingly isotropic with pressure. As already mentioned and as expected, the drift acquired by the ions at the sheath-presheath boundary [Fig. 8(d) (iii)] is much smaller at higher than at lower pressures.

To summarize, Figs. 5–8 have shown the evolution of the perpendicular ion mean energy and of the isotropic behavior of the velocity distribution while ions travel through the presheath, respectively. Figure 9 shows perpendicular ion energy distribution functions (IEDFs) at the sheath-presheath boundary for the same neutral gas pressures as depicted in Fig. 8. The ordinates are log scale and a function of energy so that a Maxwellian distribution yields a straight line. First, it should be noted that the IEDFs in the center of the discharge are not reported here as, irrespective of the pressure, they are Maxwellian distributions at the temperature of the background gas. Figure 9 allows to get a better feeling of the actual heating and see what part of the distribution is heated. Interestingly, irrespective of the pressure, the IEDFs at the sheath-presheath boundary can always be fitted by two Maxwellian distributions with two distinct temperatures a dominant cold population at the temperature of the background gas and a hotter population with a temperature of 0.1 eV. To some extent, the increase of the perpendicular energy when ions travel through the presheath is governed by the respective percentage of the cold and the hot population. Table I summarizes the ion temperature of these distributions and the fraction of the hottest population at 10 mTorr, where the

heating is maximum, 8% of the ions have a temperature of around 0.1 eV, which is almost four times the room temperature (0.026 eV). Note that at much higher pressure (several hundreds of mTorr), the bi-Maxwellian feature tends to disappear giving place to a single Maxwellian distribution.

IV. CONCLUSION

Due to the presheath, ions develop a drift velocity in the direction of the walls. At low pressure (<1 mTorr), the energy distribution function of the ions traveling through the presheath is a drifting Maxwellian that remains essentially isotropic. At higher pressure (>5 mTorr), the acceleration of the ions through the presheath is accompanied by collisions with neutrals, leading to an increase of the energy in the perpendicular direction and also to a net heating of the ion distribution function. The heating is maximum when the presheath is moderately collisional and leads to a distinctly anisotropic ion velocity distribution. In this case, the perpendicular ion energy distribution function is bi-Maxwellian: a cold population at room temperature dominates and a hotter population at 0.1 eV, representing almost 10% of the ions, is observed at the sheath-presheath boundary. When the presheath is very collisional, the ion mean energy is such that ion-neutral collisions are dominated by isotropic collisions leading to relatively isotropic ion velocity distribution functions.

The results of the present modeling scheme imply that perpendicular ion heating from presheath collisions, even in the intermediate pressure range around 8 mTorr where heating is at its most extreme, remains relatively small. Nevertheless, the issue investigated in the present paper, in addition to being interesting in itself, is of particular relevance for several practical applications such as etching, where the ion angular distribution function can have a decisive influence on the shape of the trenches as pointed out by Zheng

et al.,²⁷ or in plasma focused ion beams whose brightness is proportional to the inverse of the perpendicular ion temperature.

- ¹K.-U. Riemann, J. Phys. D **24**, 493 (1991).
- ²I. Langmuir, Phys. Rev. **33**, 954 (1929).
- ³L. Tonks and I. Langmuir, Phys. Rev. **34**, 876 (1929).
- ⁴D. Bohm, *Minimum Ionic Kinetic Energy for a Stable Sheath* (McGraw-Hill, New York, 1949).
- ⁵E. R. Harrison and W. B. Thompson, Proc. Phys. Soc. London **74**, 145 (1959).
- ⁶K.-U. Riemann, Phys. Fluids **24**, 2163 (1981).
- ⁷P. N. Hu and S. Ziering, Phys. Fluids **9**, 2168 (1966).
- ⁸R. N. Franklin, J. Phys. D **22**, 860 (1989).
- ⁹K.-U. Riemann, Phys. Fluids B **1**, 961 (1989).
- ¹⁰K.-U. Riemann, Phys. Plasmas **4**, 4158 (1997).
- ¹¹L. Oksuz and N. Hershkowitz, Phys. Rev. Lett. **89**, 145001 (2002).
- ¹²H. B. Smith, Tech. Rep., Space Plasma & Plasma Processing, The Australian National University, Canberra, 2002.
- ¹³J. P. Verboncoeur, M. V. Alves, V. Vahedi, and C. K. Birdsall, J. Comput. Phys. **104**, 321 (1993).
- ¹⁴O. Sutherland, Ph.D. thesis, The Australian National University, Canberra, 2004.
- ¹⁵R. W. Hockney and J. W. Eastwood, *Computer Simulation Using Particles* (IOP, Bristol, 1988).
- ¹⁶C. K. Birdsall and A. B. Langdon, *Plasma Physics via Computer* (McGraw-Hill, New York, 1985).
- ¹⁷A. Meige, Ph.D. thesis, The Australian National University, Canberra and Université Paul Sabatier, Toulouse, 2006.
- ¹⁸W. H. Press, S. A. Teukolsky, W. T. Vetterling, and B. P. Flannery, *Numerical Recipes in C: The Art of Scientific Computing* (Cambridge University Press, New York, 1992).
- ¹⁹G. J. M. Hagelaar, "How to normalize the density of Boltzmann electrons in a transient self-consistent plasma model," J. Comput. Phys. (unpublished).
- ²⁰A. V. Phelps, J. Appl. Phys. **1994**, 747 (1994).
- ²¹A. V. Phelps, J. Phys. Chem. Ref. Data **20**, 557 (1991).
- ²²H. R. Skullerud, Br. J. Appl. Phys. **1**, 1567 (1968).
- ²³K. Nanbu and Y. Kitatani, J. Phys. D **28**, 324 (1995).
- ²⁴V. Vahedi and M. Surendra, Comput. Phys. Commun. **87**, 179 (1995).
- ²⁵R. N. Franklin, J. Phys. D **37**, 1342 (2004).
- ²⁶M. A. Lieberman and A. J. Lichtenberg, *Principles of Plasma Discharges and Materials Processing*, 2nd ed. (Wiley Interscience, New York, 2005).
- ²⁷J. Zheng, R. P. Brinkmann, and J. P. McVittie, J. Vac. Sci. Technol. A **13**, 859 (1995).